applied sciences

MDPI

Article

Dung Beetle Optimized Fuzzy PID Algorithm Applied in Four-Bar Target Temperature Control System

Wenxiao Cao [1], Zilu Liu [2,*], Hongfei Song [2,*], Guoming Li [2] and Boyu Quan [2]

[1] School of Electronic Information Engineering, Changchun University of Science and Technology, Changchun 130022, China; caowx@cust.edu.cn
[2] School of Optoelectronic Engineering, Changchun University of Science and Technology, Changchun 130022, China; 2021100332@mails.cust.edu.cn (G.L.); 2021100338@mails.cust.edu.cn (B.Q.)
* Correspondence: 2021100439@mails.cust.edu.cn (Z.L.); shf@cust.edu.cn (H.S.)

Featured Application: This study is mainly applied to the MRTD tester and improves the four-bar target to enhance the detection accuracy of the MRTD tester. Additionally, MRTD is an important parameter for infrared thermal imaging cameras, contributing to improving their accuracy. Furthermore, the dung beetle optimized fuzzy PID parameters can be applied to most control systems, enabling stable tracking of abrupt commands and compensating for the deficiencies of traditional PID control.

Abstract: With the widespread application of infrared thermal imagers in various fields, the demand for thermal imagers and their performance parameter testing equipment has increased significantly. There are particularly high demands on the detection accuracy of minimum resolvable temperature difference (MRTD) testers. Traditional MRTD testers have an issue with the four-bar target temperatures being easily affected by the external environment, resulting in non-uniform temperatures and imprecise detection results. This paper proposes an improvement to the four-bar targets by making them temperature-controllable. Temperature is controlled by installing thermoelectric coolers (TECs) and thin-film platinum resistors at the center and periphery of the four-bar targets with different spatial frequencies. The dung beetle algorithm is used to optimize fuzzy PID parameters to regulate the TEC's heating and cooling, improving the overall temperature uniformity of the four-bar targets. Temperature simulations of the four-bar targets were conducted on the COMSOL platform, with the control part simulated on the Simulink platform. The simulation results show that, compared to traditional PID, the fuzzy PID controller reduces overshoot by approximately 3.6%, although the system still exhibits mild oscillations. The fuzzy PID controller optimized by the dung beetle optimization (DBO) algorithm, in comparison to standard fuzzy PID, reduces the settling time by about 40 s and lowers overshoot by around 7%, with oscillations in the system nearly disappearing. Comparing the fuzzy PID optimized by the particle swarm optimization (PSO) algorithm with the fuzzy PID optimized by the DBO algorithm, the DBO-based controller shows shorter rise and settling times, further illustrating the superiority of the fuzzy PID control optimized by the dung beetle algorithm. This provides a theoretical foundation for improving the accuracy of MRTD detector measurements. Finally, experimental verification was carried out. The experimental results indicate that DBO (drosophila-based optimization) has significant advantages, and its optimized results are closer to the actual values.

Keywords: dung beetle optimized; PID; minimum resolvable temperature difference; four-bar target

check for updates

Citation: Cao, W.; Liu, Z.; Song, H.; Li, G.; Quan, B. Dung Beetle Optimized Fuzzy PID Algorithm Applied in Four-Bar Target Temperature Control System. *Appl. Sci.* **2024**, *14*, 4168. https://doi.org/10.3390/app14104168

Academic Editors: Chang-Hua Lien, Chia-Hung Lin, Chao-Lin Kuo and Neng-Sheng Pai

Received: 1 March 2024
Revised: 10 May 2024
Accepted: 12 May 2024
Published: 14 May 2024

Copyright: © 2024 by the authors. Licensee MDPI, Basel, Switzerland. This article is an open access article distributed under the terms and conditions of the Creative Commons Attribution (CC BY) license (https://creativecommons.org/licenses/by/4.0/).

1. Introduction

Infrared thermal imagers utilize the principles of infrared technology to measure the infrared radiation energy emitted from the surface of an object and convert the temperature distribution of the object's surface into a vivid and intuitive thermal image. Due to their

rapid response time, wide measurement range, non-contact measurement capability, and visually intuitive results, infrared thermal imagers are extensively used in military, medical, industrial, and other fields [1,2]. Infrared thermal imagers are not only a key factor in modern military confrontations but have also gained increasing attention in civilian applications. They are now employed in the diagnosis of cancer, the monitoring of diabetes [3,4], and the surveillance and thermal fault analysis of equipment in power fields [5].

With the widespread application of infrared thermal imagers, higher demands have been placed on these devices. The minimum resolvable temperature difference (MRTD) is a critical standard for evaluating the performance of infrared thermal imaging systems [6]. Therefore, enhancing the detection accuracy of MRTD testers is a key focus in improving the precision of infrared thermal imagers [7]. Currently, the general method for measuring MRTD involves the following steps: a four-bar target with a high aspect ratio of 7:1 is placed against a uniform background, and the temperature difference between the target and the background is either increased or decreased. The temperature difference at which the human eye can just resolve the image of the four-bar target displayed on the system's monitor corresponds to the MRTD value at that specific spatial frequency. To eliminate test errors caused by zero drift, the average of the positive and negative temperature differences is typically taken as the final test result. Traditional four-bar targets are depicted in Figure 1 [8].



Figure 1. Four-bar target.

In recent years, researchers have proposed improvements to the MRTD testing method. These improvements shift from traditional human visual observation to the use of CCD cameras [9] by measuring the modulation transfer function (MTF), calculating MRTD using the noise equivalent temperature difference (NETD) [10], and employing neural networks [11]. However, compared to traditional methods, objective measurement techniques struggle to achieve higher accuracy. Although these methods reduce labor costs, they are not suitable for high-precision measurements. In related research, the temperature of the four-bar target is easily influenced by external environmental conditions and the temperature of the blackbody, leading to uneven thermal distribution across the target. This unevenness can prevent the achievement of consistent test conditions across the entire target surface, resulting in imprecise test outcomes and failing to accurately reflect the actual performance of the thermal imaging system. This study proposes an improvement to the four-bar target by employing intelligent optimization algorithms to control the temperature at various points on the target, ensuring uniform temperature distribution across the entire target.

In recent studies, researchers have conducted in-depth investigations into various intelligent optimization algorithms for control systems. Jintao Meng et al. [12] proposed a temperature control system for a vacuum annealing furnace based on a Genetic Algorithm-optimized fuzzy PID (GA-Fuzzy-PID). Compared to traditional control methods, this system shows significant advantages in temperature accuracy, rise time, and overshoot con-

trol. Jiaxiao [13] Chen et al. also proposed a control method combining genetic algorithms with fuzzy PID. However, the high computational complexity of genetic algorithms might lead to insufficient real-time performance. Hao Tang et al. [14] addressed the nonlinearity and hysteresis issues in lychee preservation equipment by introducing a particle swarm optimization-enhanced fuzzy PID (PSO-Fuzzy PID) control method. The results indicated that the PSO-Fuzzy PID scheme significantly reduced disturbance adjustment time and eliminated overshoot, exhibiting superior control performance, although it might fall into local optima during computation, leading to inaccurate parameter adjustments. Mingsan Ouyang et al. [15] introduced an improved sparrow search algorithm (ISSA) to optimize PID parameters in the temperature control process of a continuous stirred tank reactor (CSTR). Experimental results showed improved transient and steady-state performance of the reactor temperature control with good precision and robustness, although the convergence was poor after enhancing the capability to escape local minima. Ahmad Nor Kasruddin [16] Nasir et al. proposed a novel hybrid strategy combining the spiral dynamics algorithm (SDA) with the bacterial foraging algorithm (BFA) to design a fuzzy controller for flexible manipulators, but its slow convergence rate made it unsuitable for real-time systems. Aiguo Jin et al. [17] designed a temperature control system for infant radiant warmers using a Kalman filter-based fuzzy PID (KFPID) algorithm. Experimental results demonstrated shorter adjustment times, nearly zero overshoot, and smaller steady-state errors compared to control systems without this algorithm, particularly showing effectiveness in noise suppression. Amit Kumar et al. [18] introduced a novel hybrid controller that combines the fuzzy PID with PID optimized by the whale optimization algorithm (WOA), showing excellent performance in frequency regulation in hybrid power systems, though the method has a slow convergence rate and is sensitive to initial settings. Zhe Sun et al. [19] proposed a fuzzy logic power system stabilizer (FLPSS) based on the grey wolf optimization algorithm (GWO). Compared to traditional stabilizers and optimization algorithms, it provided faster system response time and higher damping of oscillations, although its robustness was less satisfactory. Alok Kumar Mishra et al. [20] proposed a novel estimation algorithm—the robust extended Kalman filter—to estimate the fundamental phase component of the reference current and employed a novel adaptive fuzzy PID controller to generate the maximum value of the reference current. All controller parameters were optimized using an improved football game optimization (IFGO) technique. Additionally, the sliding mode control (SMC) technique was used to generate switching pulses for the voltage source converter (VSC). Haiyu Zhang et al. [21] introduced a gas distribution system based on a fuzzy PID controller, where the system's mathematical model was built using the step response method, and the gas distribution control process was optimized. However, this method is subject to the influence of human factors on parameter adjustments.

To address these challenges, this paper improves the four-bar target by installing thermoelectric coolers (TECs) and thin-film platinum resistors on its surface to lower the central temperature and elevate the peripheral temperature, thereby maintaining consistent temperature across the entire plane. A high-temperature uniformity target provides an accurate and consistent thermal field, which allows for more precise measurement of the MRTD value of infrared thermal imagers. In controlling the temperature of the four-bar target, this paper introduces the dung beetle algorithm for online optimization of quantization and proportionality factors, seeking optimal solutions for each parameter. This significantly enhances the accuracy and reliability of MRTD detection, thereby positively impacting the performance evaluation of thermal imaging products. The dung beetle algorithm is a heuristic optimization algorithm based on biomimetic principles and inspired by the behavior of dung beetles when searching for food and shelter. Compared to other algorithms, the dung beetle algorithm first utilizes swarm intelligence to search the entire solution space, which helps in discovering the global optimum and improving the overall performance of the control system. Additionally, the dung beetle algorithm has a certain degree of adaptability, allowing it to dynamically adjust its search strategy based on changes in the

search space. This enables the algorithm to cope with changes and uncertainties during the control system operation, thereby enhancing the system's stability and robustness. Lastly, the dung beetle algorithm usually features high convergence speed and search efficiency, enabling it to find better solutions within a relatively short time. This is advantageous in real-time control systems for rapid parameter adjustment to accommodate dynamic changes in the system.

The four-rod target in a conventional MRTD detector is subject to external influences, which can lead to the problem of low temperatures around the perimeter and high temperatures in the center. In this study, for the first time, a highly uniform temperature control strategy is proposed for the temperature control of the four-rod target in MRTD detection instruments to reduce the influence of the outside world on its temperature uniformity. Compared with the existing technology, this paper adopts an advanced intelligent algorithm dung beetle optimization algorithm to optimize the fuzzy PID parameters, which significantly improves the performance of MRTD detection, and the algorithm provides a reference value for all temperature control systems with high precision requirements. It fills the gap in existing research and provides a new research direction and important theoretical basis for the development of future temperature control technology.

2. Principles and Methods

2.1. Improving the Four-Bar Target

This research is focused on the temperature control of the four-bar target to minimize interference from the external environment. The traditional four-bar target has a problem with higher temperatures at the center and lower temperatures around the edges. To improve this situation, TECs (thermoelectric coolers) have been placed at both the center and the small square positions around the perimeter of the four-bar target to achieve temperature control, as shown in Figure 2. By coordinating the operation of multiple TECs, the objective was to lower the temperature at the center of the four-bar target and raise the temperature around the edges, thereby achieving an overall temperature balance. Additionally, thin-film platinum resistors were used to measure the temperature at various points to ensure consistency across all points and to detect the maximum temperature difference across the entire plane. The measured temperature values were fed back to a PID controller, which formed a closed-loop system, to improve the temperature uniformity of the four-bar target, thereby enhancing the detection accuracy of the MRTD tester.

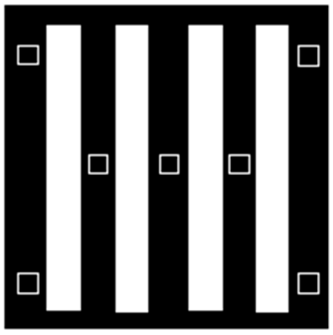


Figure 2. Improved four-bar target.

2.2. Establishment of Transfer Functions

A TEC (thermoelectric cooler) [22] is a type of thermoelectric device based on the Peltier effect, where direct current passing through a thermocouple made up of two semiconductor materials can cause one side of the thermocouple to absorb heat while the other side releases heat. Although a TEC is an electric current transducer, its operating current and voltage are related to its internal resistance. The operating voltage of a TEC can also reflect its operating state, and since voltage sources are more common, the analysis of the TEC system is based on the input voltage. The heating system is a first-order inertia system with delay.

By first transforming the heat balance equation of a first-order inertia system using Laplace transforms, the relationship between temperature change and voltage change in the system can be obtained:

$$\begin{cases} T\frac{d\Delta T}{dt} + \Delta T = K\Delta u \\ Ts\Delta T(s) + \Delta T(s) = K\Delta U(s) \\ G(s) = \frac{\Delta T(s)}{\Delta U(s)} = \frac{K}{Ts+1} \end{cases} \quad (1)$$

where $\Delta T(s)$ is the temperature change, $\Delta U(s)$ is the voltage change, K is the system gain, T is the time constant, and s is the complex variable, which in this case is the differential operator. The model of the controlled object in the temperature control system can be represented by a first-order delay function, and after calculation, the transfer function of this article is as follows [23]:

$$G(s) = \frac{K}{Ts+1}e^{-\tau s} = \frac{0.6}{60s+1}e^{-6s} \quad (2)$$

where K is the system gain, T is the time constant, and τ is the time delay.

2.3. Fuzzy PID Control

Combining fuzzy control theory with classical PID control forms a fuzzy PID controller, where the fuzzy algorithm can play an auxiliary optimization role. Based on a conventional PID controller, the deviation e and the rate of change of the deviation ec are used as input variables to the fuzzy controller, and the classical PID's three incremental correction values Kp, Ki, Kd serve as the output of the fuzzy controller, resulting in a two-input and three-output structure [23,24]. The principle block diagram of a fuzzy PID control system is shown in Figure 3.

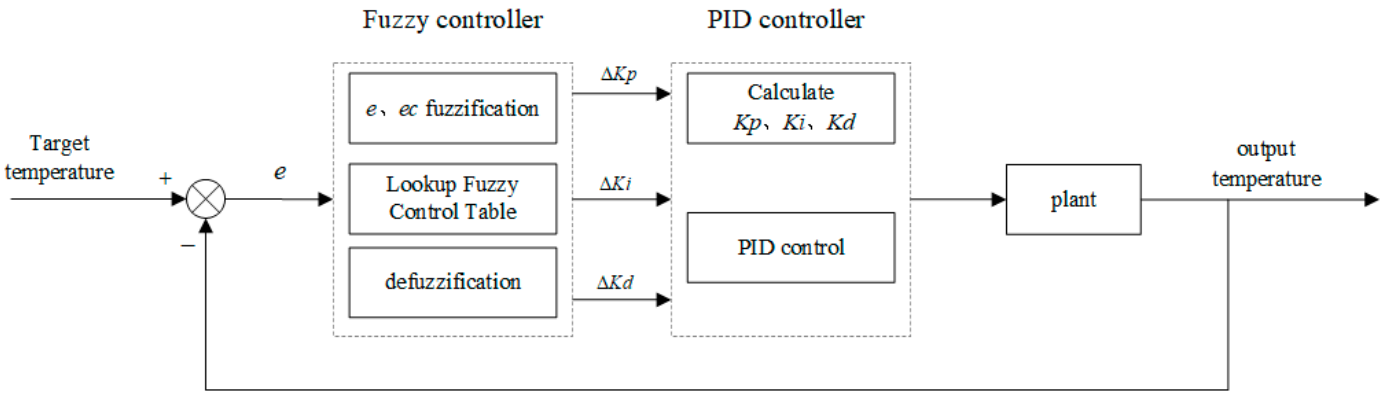


Figure 3. The principle block diagram of a fuzzy PID control system.

According to the characteristics of the temperature control system in this system, all variables are described using trimf (triangular membership functions), as shown in Figures 4 and 5:

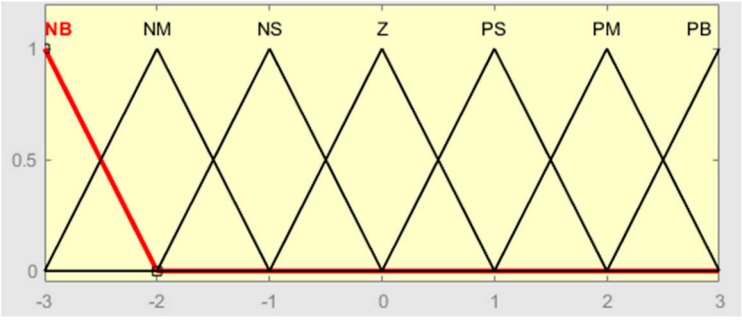


Figure 4. *e* and *ec* membership function diagram.

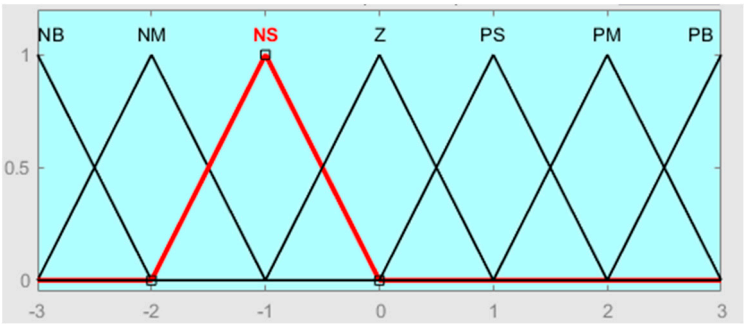


Figure 5. *Kp*, *Ki*, and *Kd* membership function diagram.

In this paper, the inputs are the temperature deviation *e* and the rate of change of temperature deviation *ec*, which are subject to fuzzification. The fuzzy subsets are defined as NB, NM, NS, ZO, PS, PM, and PB. Furthermore, a fuzzy rule table is deduced as shown in Tables 1–3:

Table 1. *Kp* fuzzy rules.

e	*ec*						
	NB	**NM**	**NS**	**ZO**	**PS**	**PM**	**PB**
NB	PB	PB	PM	PM	PM	PB	PB
NM	PB	PB	PM	PM	PM	PB	PB
NS	PM	PS	PS	ZO	PS	PM	PM
ZO	PM	PS	PS	ZO	PS	PM	PM
PS	PM	PM	PS	PS	PS	PM	PM
PM	PB	PB	PM	PM	PM	PM	PB
PB	PB	PB	PM	PM	PM	PB	PB

Table 2. *Ki* fuzzy rules.

e	*ec*						
	NB	**NM**	**NS**	**ZO**	**PS**	**PM**	**PB**
NB	NB	NB	PM	PM	PM	NB	NB
NM	NB	NB	PS	PS	PS	NB	NB
NS	NM	NM	NS	NS	NS	NM	NM
ZO	NM	NM	NS	NS	NS	NM	NM
PS	NM	NM	NS	NS	NS	NM	NM
PM	NB	NB	PS	PS	PM	NB	NB
PB	NB	NB	PM	PM	PM	NB	NB

Table 3. *Kd* fuzzy rules.

e	*ec*						
	NB	**NM**	**NS**	**ZO**	**PS**	**PM**	**PB**
NB	PB	PB	PM	PM	PM	PB	PB
NM	PB	PM	PS	PS	PS	PM	PB
NS	PM	PS	ZO	ZO	ZO	PS	PM
ZO	PM	PS	ZO	ZO	ZO	PS	PM
PS	PM	PS	ZO	ZO	ZO	PS	PM
PM	PB	PM	PS	PS	PM	PM	PB
PB	PB	PB	PM	PM	PM	PB	PB

The de-blurring is performed using a weighted averaging method, with the results automatically generated by the fuzzy PID controller, as shown in Figure 6. The values of *e* and *ec* can be manually input to verify the magnitude changes of Δ*Kp*, Δ*Ki*, and Δ*Kd*.

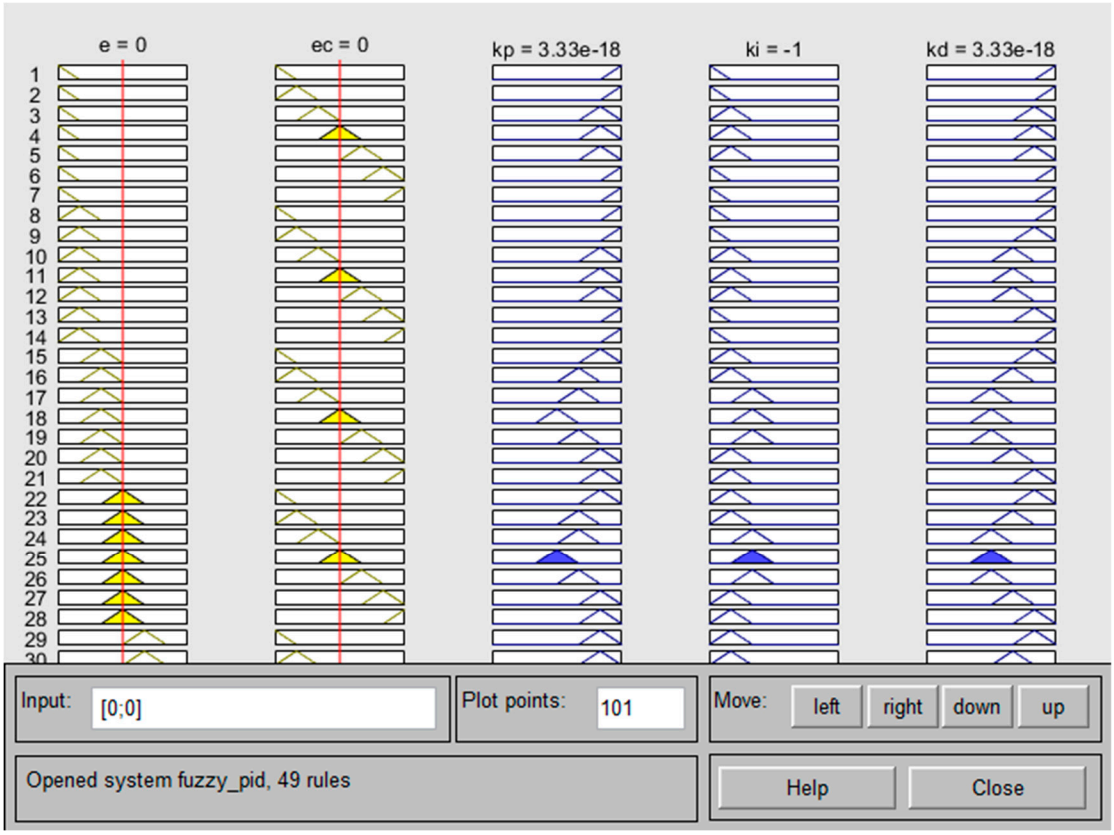


Figure 6. Fuzzy rule editor.

According to fuzzy rules, the PID controller dynamically adjusts the proportional (P), integral (I), and derivative (D) gains. When the error e is large, *Kp* is set to a higher value, *Ki* is set relatively smaller, and *Kd* is moderately smaller. When the errors *e* and *ec* are moderate, *Kp* is set to a lower value. The values of *Ki* and *Kd* need to be moderate. In cases of larger errors, for better robustness, *Kp* is set to a smaller value, *Ki* is increased to prevent oscillations, and *Kd* is set to a moderate level.

2.4. Dung Beetle Optimize

The dung beetle optimization algorithm (DBO) [25–27] is a novel swarm intelligence optimization algorithm proposed on 27 November 2022 by Professor Bo Shen's team at Donghua University. By observing and studying the habits of dung beetles, they discovered the irreplaceable role of dung balls in the dung beetle's survival. Dung balls not only serve as the breeding ground for larvae but also provide the necessary food for their sustenance. Mathematical modeling of behaviors such as rolling, dancing, foraging, stealing, and reproduction led to the development of the dung beetle optimization algorithm, which is characterized by its strong optimization ability and fast convergence rate.

The dung beetle optimization algorithm mainly includes four processes: rolling, breeding, foraging, and stealing. The dung beetle population is divided into four parts: the ball-rolling dung beetles, the breeding balls, the young dung beetles, and the thieving dung beetles [28,29]. Ball-rolling dung beetles determine their movement direction by the sun, moon, or polarized light, choosing safer locations to forage. Breeding balls are born in the safe locations selected by the ball-rolling dung beetles. Young dung beetles, which eventually grow into adults, search for food in the optimal foraging areas. Thieving

dung beetles forage or steal dung balls based on known optimal foraging areas and the locations of other companions. The optimization process of the DBO algorithm for fuzzy PID control mainly has six steps [30]: (1) initialize the dung beetle population and DBO algorithm parameters; (2) calculate the fitness values of all dung beetles' positions based on the objective function; (3) update the positions of all dung beetles; (4) check if any updated dung beetles have gone out of bounds; (5) update the current optimal solution and its fitness value; and (6) repeat the above steps until t reaches the maximum number of iterations, after which the global optimum value and the optimal solution are output.

Here are the specific update processes for the four different dung beetle positions:

2.4.1. Roll-Ball Dung Beetle

The roll-ball dung beetle navigates with the sun to ensure the dung ball rolls in a straight path. Natural factors like light intensity and wind can influence the roll-ball dung beetle's trajectory [31]. The position update for the roll-ball dung beetle can be expressed as follows:

$$x_i(t+1) = x_i(t) + \alpha \times k \times x_i(t-1) + b \times \Delta x \tag{3}$$

$$\Delta x = |x_i(t) - X^w| \tag{4}$$

where t represents the current iteration number; $xi(t)$ represents the position information of the i-th dung beetle at the t-th iteration; α is a natural coefficient that indicates whether to deviate from the original direction, assigned -1 or 1 based on probability; $k \in (0, 0.2)$ represents the deviation coefficient; $b \in (0, 1)$ represents a constant, with k and b set to 0.1 and 0.3, respectively; X^w denotes the global worst position; and Δx is used to simulate changes in light intensity. The movement direction of the dung beetle is shown in Figure 7.

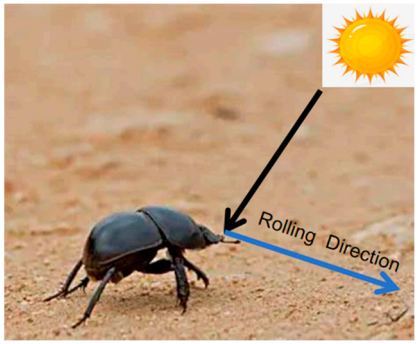


Figure 7. Dung beetle movement direction.

The updated formula for the dancing position of a dung beetle on a dung ball when it encounters an obstacle and needs to choose a new route to continue moving forward can be represented as follows:

$$x_i(t+1) = x_i(t) + \tan(\theta)|x_i(t) - x_i(t-1)| \tag{5}$$

where $\theta \in [0, \pi]$ represents the deviation angle, and when θ is equal to 0, $\pi/2$, or π, the position of the dung beetle will not be updated.

2.4.2. Brood Ball

The brood ball utilizes a boundary selection strategy to simulate the oviposition area of a female dung beetle. The definition of the oviposition area is as follows:

$$Lb^* = \max(X^* \times (1 - R), Lb) \tag{6}$$

$$Ub^* = \min(X^* \times (1 + R), Ub) \tag{7}$$

where X^* represents the current local best position; Lb^* and Ub^* represent the lower and upper bounds of the oviposition area, respectively; $R = 1 - t/Tmax$, where $Tmax$ represents the maximum number of iterations; and Lb and Ub represent the lower and upper bounds of the optimization problem.

As indicated by the above formula, the oviposition area is dynamically changing. Therefore, during the iteration process, the position of the brood ball is also dynamically changing. The position of the brood ball is defined as follows:

$$B_i(t+1) = X^* + b_1 \times (B_i(t) - Lb^*) + b_2 \times (B_i(t) - Ub^*) \quad (8)$$

where $B_i(t)$ represents the position information of the i-th brood ball during the t-th iteration; b_1 and b_2 are two independent random vectors of size $1 \times D$; and D represents the dimension of the optimization problem.

2.4.3. Scout Dung Beetle

After being born, the scout dung beetle searches for food in the best foraging area. The definition of the best foraging area is as follows:

$$Lb^* = \max\left(X^b \times (1 - R), Lb\right) \quad (9)$$

$$Ub^* = \max\left(X^b \times (1 + R), Ub\right) \quad (10)$$

where X^b represents the current local best position, and Lb^b and Ub^b represent the lower and upper bounds of the best foraging area. Therefore, the position of the scout dung beetle is updated as follows:

$$x_i(t+1) = x_i(t) + C_1 \times \left(x_i(t) - Lb^b\right) + \mathbf{C}_2 \times \left(x_i(t) - Ub^b\right) \quad (11)$$

where $X_i(t)$ represents the position information of the i-th scout dung beetle during the t-th iteration, C_1 represents a random number following a normal distribution, and $C_2 \in (0,1)$ represents a random vector.

2.4.4. Thief Dung Beetle

The thief dung beetle steals dung balls from other dung beetles. As derived from the above equation, X^b is the best location for competing for food. Therefore, the position information of the thief dung beetle is updated as follows:

$$x_i(t+1) = X^b + S \times g \times (|x_i(t) - X^*| + |x_i(t) - X^b|) \quad (12)$$

where $x_i(t)$ represents the position information of the i-th thief dung beetle during the t-th iteration, g represents a random vector of size $1 \times D$ following a normal distribution, and S represents a constant value.

The workflow diagram of optimizing fuzzy PID parameters using the dung beetle optimization algorithm is shown in Figure 8.

The optimization principle diagram of the dung beetle optimization algorithm for tuning fuzzy PID parameters is shown in Figure 9.

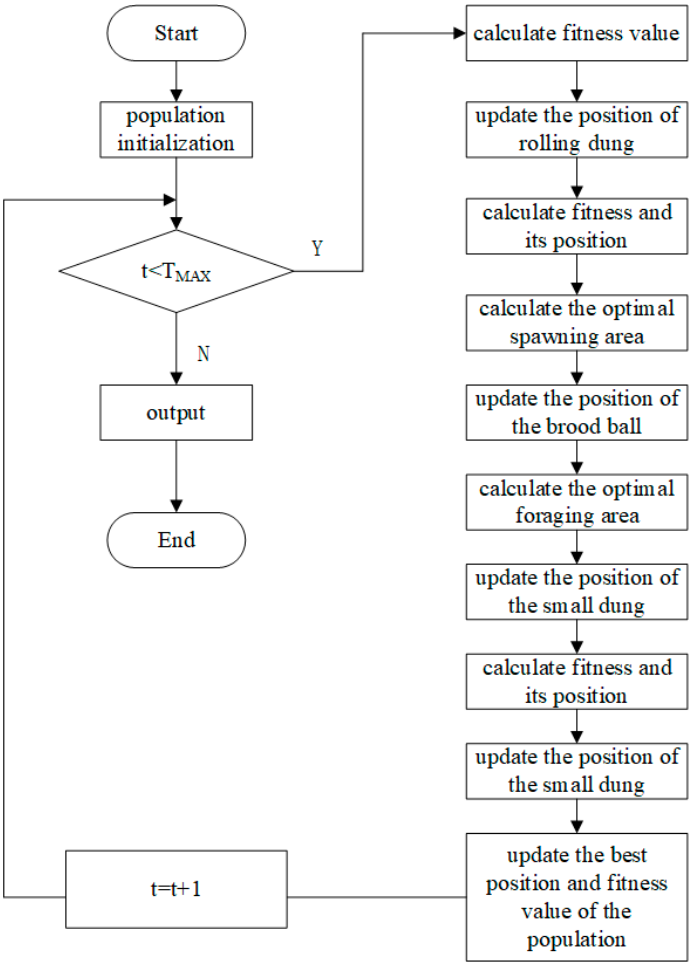


Figure 8. Flowchart of dung beetle optimization algorithm.

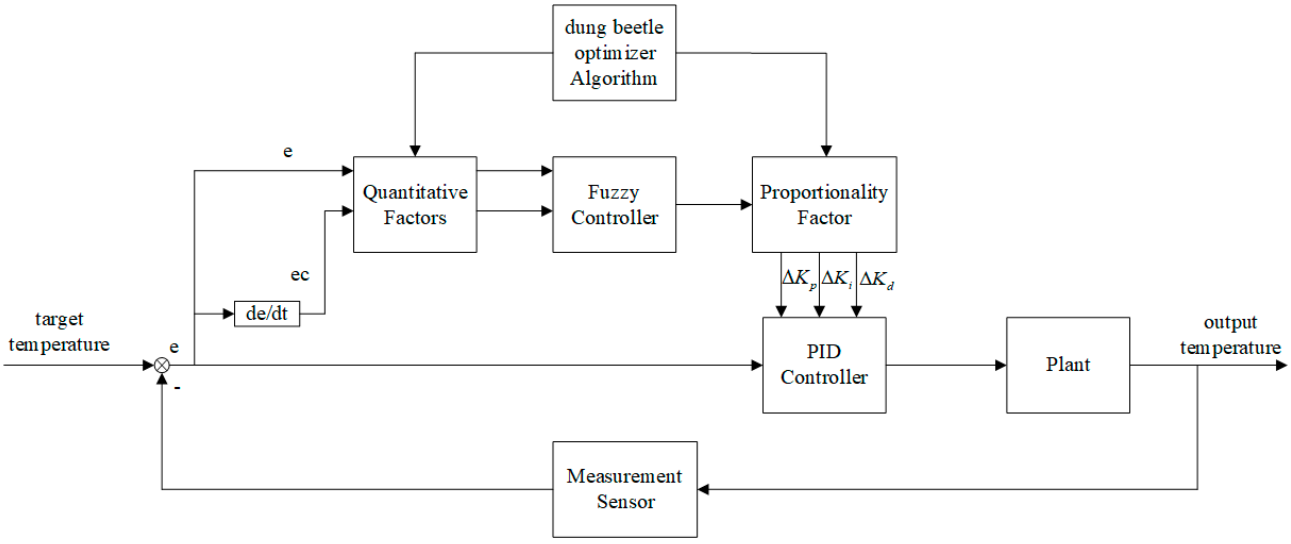


Figure 9. System principle block diagram.

2.5. Applying DBO to Adjust Controller Parameters

Three steps were conducted to connect the position of the dung beetle to controller parameter adjustments and to associate the DBO's fitness function with the fitness function for control problems.

First, the controller parameter vector was set as $P = [Kp, Ki, Kd]$, where Kp, Ki, and Kd are the proportional, integral, and derivative gains of the PID controller, respectively.

Second, the position of the dung beetle X was mapped to the controller parameters P, where each dung beetle represents a set of possible PID parameters. Updates to the position of the dung beetle will directly affect the adjustments of the PID parameters. Use a linear mapping function $f(X) = aX + b$, where a and b are mapping coefficients. These coefficients can be adjusted based on the desired range of controller parameters.

Lastly, the fitness function for the control problem was defined by choosing the integral of time-weighted absolute error (ITAE) as the fitness function for the control issue, defined as $ITAE = \int_0^{t_f} t \cdot |e(t)| dt$, where $e(t)$ is the system's error signal, and t_f is the final time.

3. Results

3.1. Dung Beetle Optimization Fuzzy PID Simulation

Having outlined the optimization process of the dung beetle optimization algorithm, we first initialized the parameter settings, defined the quantization factor and the scaling factor, set the population size to 50, and set the maximum number of iterations to 100. By writing the main program code for the dung beetle optimization and the code for the fitness calculation subfunction and compiling and running on MATLAB2019 software, we obtained the evolution process curves of the quantization factor and the scaling factor, as shown in Figures 10 and 11.

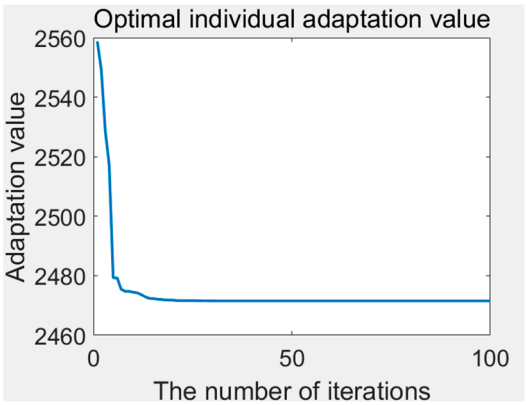


Figure 10. Iteration curve.

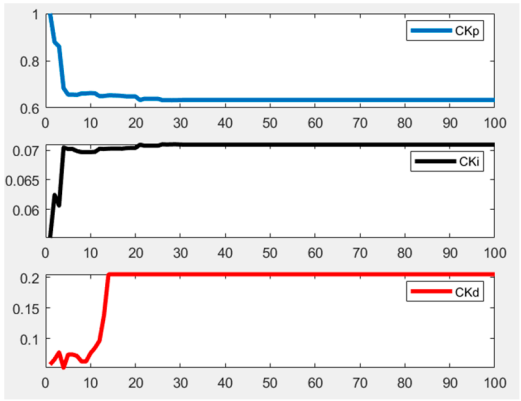


Figure 11. Proportional factor optimization curve.

After running 30 iterations and recording the final fitness values of each run, the statistical analysis results are presented in Table 4.

Table 4. Fitness function statistical analysis.

ITAE Average	ITAE Standard Deviation	ITAE Min	ITAE Max
2474.7133	0.3791	2474.2137	2475.6608

In the Simulink simulation platform, we construct simulation models for the dung beetle algorithm-optimized fuzzy PID control, particle swarm optimization (PSO) optimized fuzzy PID, fuzzy PID, and classical PID control to compare the effects of temperature changes. The simulation models are illustrated in Figure 12.

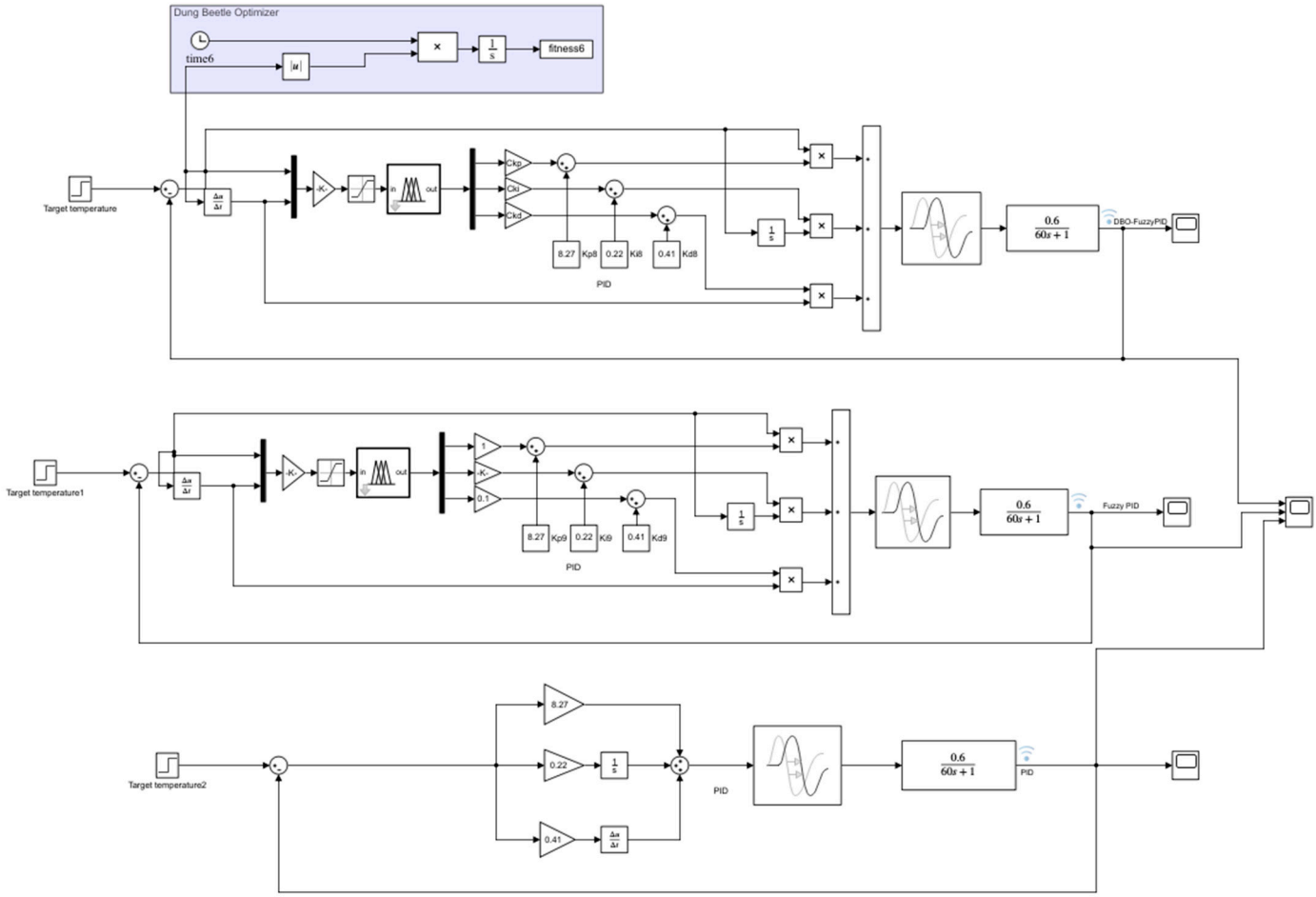


Figure 12. System simulation diagram.

By using the trial-and-error method, the following initial values of the classical PID were obtained: Kp = 8.27, Ki = 0.22, and Kd = 0.41. These values were used as the initial ones for the classical PID, fuzzy PID, particle swarm optimization (PSO) optimized fuzzy PID, and dung beetle algorithm-optimized fuzzy PID. For the fuzzy PID, after 100 iterations of optimization with the dung beetle algorithm, the most suitable scaling factor was obtained. The specific optimized values of the scaling factor are shown in Table 5.

Table 5. Optimal scaling factor values.

Optimization Objective	Ck_p	Ck_i	Ck_d
Optimization results	0.6340	0.0710	0.2050

A sensitivity study was carried out on the three parameters *Kp*, *Ki*, and *Kd*, which were varied separately to obtain different simulation results and compare them, as shown in Figure 13.

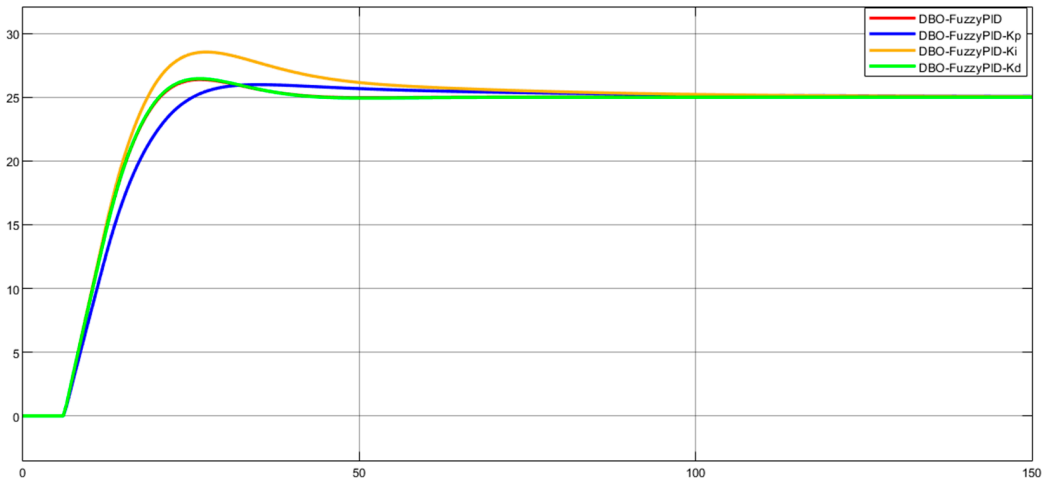


Figure 13. Sensitivity analysis of *Kp*, *Ki*, and *Kd*.

To verify the superiority of the scale factor, the initial temperature was set to 0 °C, and the target temperature was set to 25 °C. A simulation platform was constructed using MATLAB2019/Simulink to perform simulations on the temperature control system of the four-bar target in the MRTD (minimum resolvable temperature difference) tester. The simulation compared the performance of four different control strategies: traditional PID control, fuzzy PID control, particle swarm optimization of fuzzy PID, and fuzzy PID control optimized by the dung beetle optimization (DBO) algorithm. By observing key performance indicators such as heating speed, overshoot, settling time, and steady-state error, a detailed analysis of the response characteristics and temperature control effectiveness of each control strategy was conducted. The results are illustrated in Figure 14.

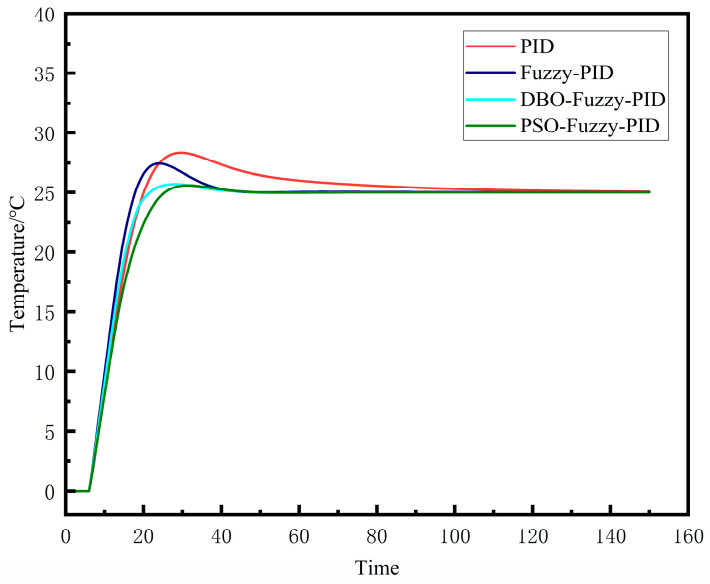


Figure 14. Comparison chart of traditional PID, fuzzy PID, particle swarm fuzzy PID, and dung beetle fuzzy PID.

By comparing these response curves, it is evident that the dung beetle optimization-enhanced fuzzy PID control exhibits superiority in aspects such as system response time,

overshoot, and oscillation effects. The simulation experiments not only confirm the importance of scale factor adjustment but also demonstrate the effectiveness of the optimization algorithm in enhancing the performance of the temperature control system, as shown in Table 6.

Table 6. Dynamic performance comparison.

	Peak Time/s	Overshoot/%	Oscillation Effect	Settling Time/s
Traditional PID	29.5	13.453%	Larger	82.5
Fuzzy PID	24	9.84%	Smaller	77
Dung beetle optimization optimized fuzzy PID	28	2.757%	Smaller	33
Particle swarm optimization of fuzzy PID	31.5	2.357%	Smaller	35

From Table 6, it can be observed that compared to traditional PID control, fuzzy PID reduces overshoot by approximately 3.6%, with the system still exhibiting mild oscillations. When comparing the optimization of fuzzy PID using the dung beetle algorithm to fuzzy PID itself, the settling time decreases by around 40 s, overshoot decreases by about 7%, and the system's oscillatory behavior is largely eliminated. Additionally, when comparing the optimization of fuzzy PID using the particle swarm optimization algorithm to that of the dung beetle algorithm, both the rise time and settling time of the particle swarm optimization are shorter, showcasing the superior performance of the bung beetle algorithm in optimizing fuzzy PID control.

The system was subjected to multiple heating and cooling simulations to analyze its stability during temperature transitions. The response curves for traditional PID control, fuzzy PID control, particle swarm optimization of fuzzy PID, and DBO-optimized fuzzy PID control are shown in Figure 15.

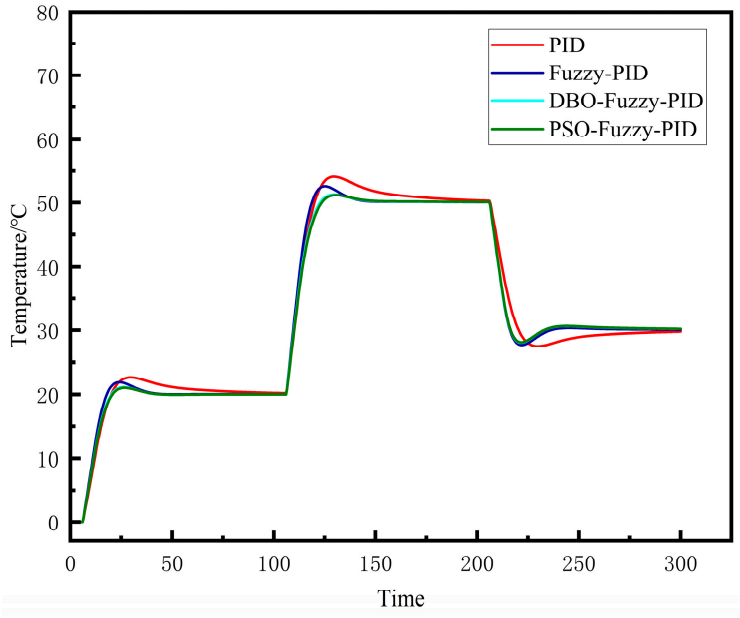


Figure 15. Comparison of results for multiple temperature jumps.

In the process of frequently changing temperatures, the DBO-optimized fuzzy PID control was capable of adjusting the temperature to the set point quickly, and the curve becomes stable after reaching the set temperature. This indicates that the algorithm still performs well even under conditions of frequent changes to the control temperature.

In the optimization of the fuzzy PID control system using the dung beetle optimization algorithm, Gaussian white noise was introduced as a disturbance for simulation analysis. The simulation results show that the system exhibits only minor fluctuations when sub-

jected to noise interference, maintaining overall stability with little impact on rise time and overshoot. The steady-state error may be slightly larger compared to the system without noise but remains within a reasonable range. Therefore, the system demonstrates strong robustness. The simulation results are shown in Figure 16.

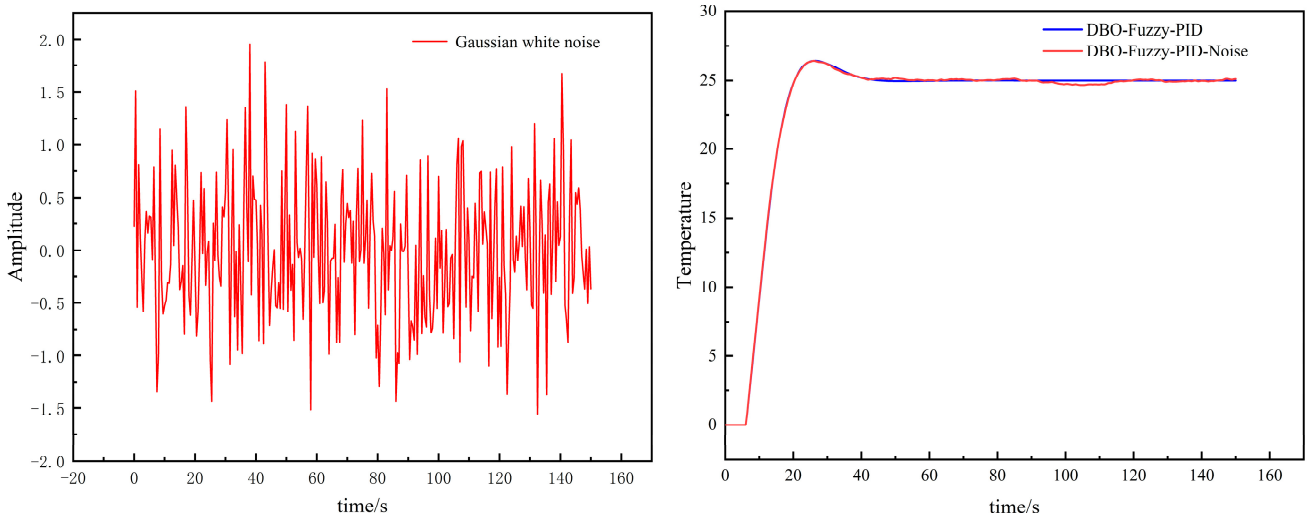
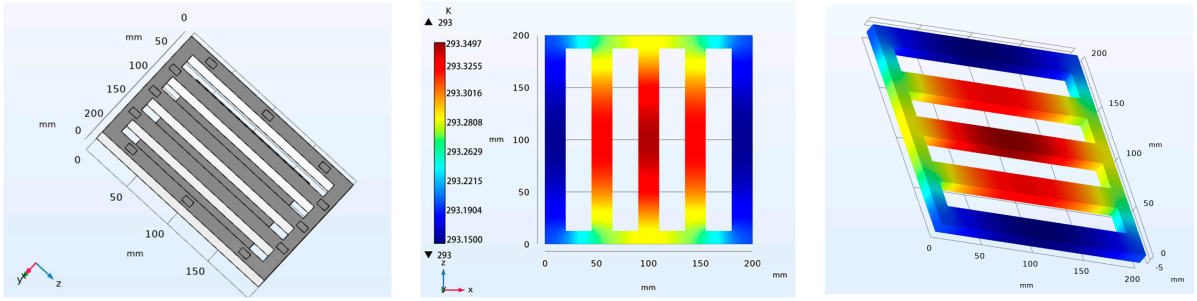


Figure 16. Results with noise interference.

3.2. COMSOL Temperature Field Simulation

When using the COMSOL [32,33] platform for temperature field simulation of the four-bar target, the traditional four-bar target exhibited an uneven overall temperature [34], with the perimeter temperature being lower than the central temperature, and a maximum temperature difference of 1.5 °C, as shown in Figure 17.

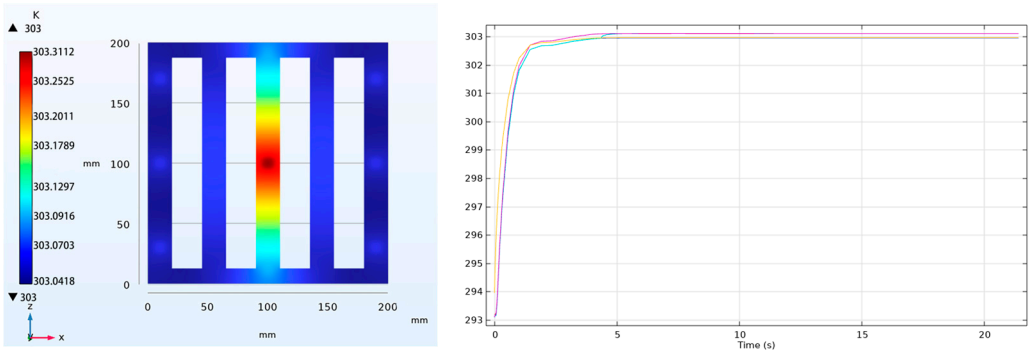


(**a**) (**b**) (**c**)

Figure 17. Traditional four-bar target temperature field distribution (**a**–**c**).

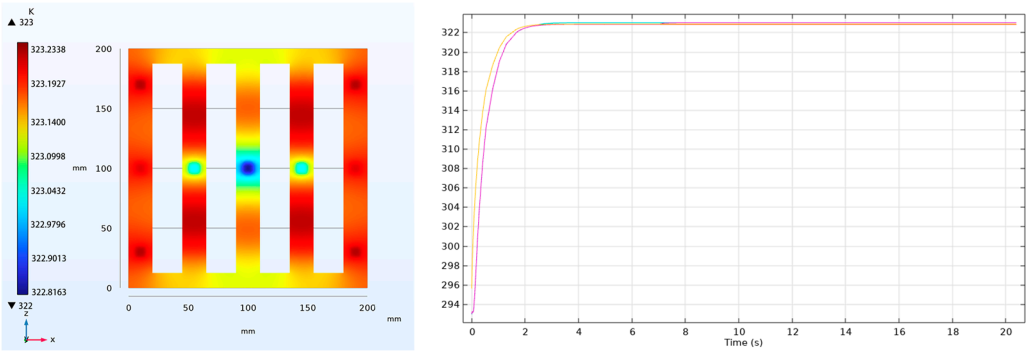
The paper proposes the installation of TECs (Thermoelectric Coolers) and thin-film platinum resistors around the perimeter and at the center of the four-bar target. Simulations of the temperature field for the improved four-bar target were conducted with an ambient temperature set at 20 °C, and the four-bar target temperatures were set at 30 °C and 50 °C, respectively. The temperature field simulations are shown in Figures 18 and 19.

Based on the results from the four groups of simulations mentioned, it can be concluded that within the same plane, the difference between the highest and lowest temperatures is less than 0.5 °C, meaning the overall temperature uniformity is better than 0.5 °C. Concerning the external environment of the target, external environmental parameters such as atmospheric ambient temperature, solar radiation, humidity, wind speed, and ground temperature can have a certain impact on the temperature of the target surface. By controlling the temperature of the four-bar target, the uniformity of the overall temperature has been improved, as shown in Table 7.



(**a**) (**b**)

Figure 18. Simulation diagram of temperature field at 30 °C (**a**,**b**).



(**a**) (**b**)

Figure 19. Simulation diagram of temperature field at 50 °C (**a**,**b**).

Table 7. Target surface temperature analysis at different set temperatures.

Ambient Temperature (K)	Four-Bar Target Temperature (K)	Maximum Value (K)	Minimum Value (K)	Temperature Difference (K)
293.15	293.15	293.3497	293.15	0.1997
	298.15	298.3303	298.0972	0.2331
	303.15	303.3112	303.0418	0.2694
	323.15	323.2338	322.8163	0.4175

3.3. Experimental Validation

Based on the above summary, both the dung beetle optimization algorithm and the particle swarm optimization algorithm have shown good results in optimizing fuzzy PID controllers. During the experimental process, identical platinum resistors were selected and individually calibrated. One set of resistors was controlled using fuzzy PID parameters optimized by the dung beetle optimization algorithm, while the other set was controlled using parameters optimized by the particle swarm optimization algorithm. Both were placed in a constant temperature bath at as similar a depth as possible. The experimental setup is shown in Figure 20.

By measuring multiple sets of data and comparing the results from both channels with those from a standard thermometer, it is evident that the outcomes optimized by the dung beetle optimization algorithm are closer to the standard thermometer readings, as shown in Figure 21.

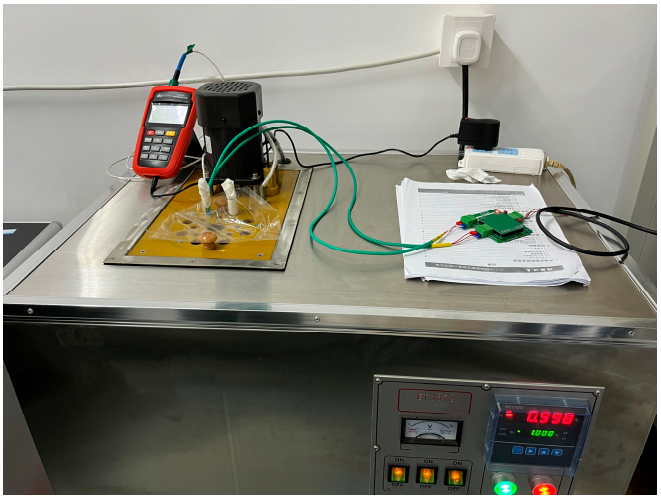


Figure 20. Experimental setup.

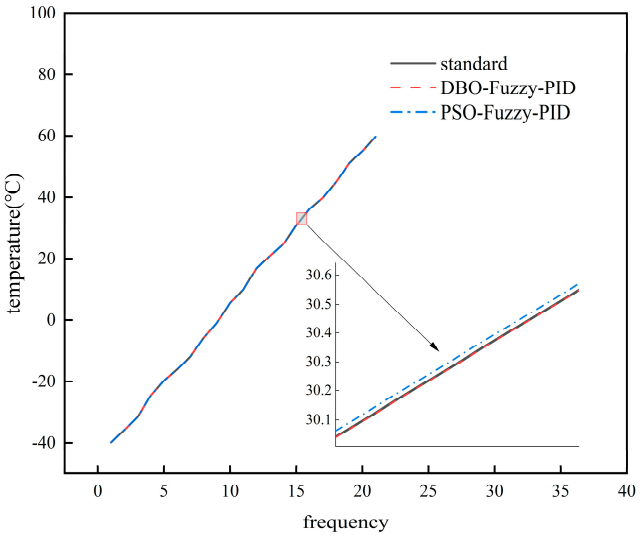


Figure 21. Measurement data.

4. Conclusions

This study conducted an in-depth investigation of the four-bar targets in MRTD (Minimum Resolvable Temperature Difference) detection instruments. Unlike traditional MRTD devices that use temperature-uncontrollable targets, this paper innovatively proposes a design for temperature-controllable four-bar targets. By installing thermoelectric coolers (TECs) and thin-film platinum resistors at the center and periphery of the targets, the precision of MRTD detection has been significantly enhanced. In terms of temperature control, the study adopts the dung beetle algorithm to optimize the temperature control system, introducing fuzzy control to dynamically adjust PID parameters online, replacing the traditional fixed parameter adjustment method, thereby improving the system's robustness and disturbance rejection capability. By optimizing the fuzzy PID controller with the dung beetle algorithm, the study approaches the problem of stable tracking of step commands with fuzzy PID, seeking the optimal real-time adjustment parameters to demonstrate the significant advantages of the fuzzy PID control after optimization with the dung beetle algorithm. On the Simulink platform, a comparative simulation analysis of DBO-optimized fuzzy PID, PSO-optimized fuzzy PID, fuzzy PID, and traditional PID was conducted. The results show that DBO-optimized fuzzy PID has notable advantages over traditional PID and fuzzy PID in terms of a lower overshoot, a shorter adjustment time, and a stronger anti-interference capability. Additionally, the study performed a simulation

analysis of the temperature field of the four-bar targets on the Comsol platform, validating the improvement in temperature uniformity, which fully meets the temperature control requirements of the four-bar targets in MRTD detection instruments, thus significantly enhancing the performance of MRTD detection.

In subsequent research, it is possible to consider using more advanced intelligent algorithms to optimize its parameters, which might lead to a better combination of parameters. Additionally, during the experimental process, more environmental factors could be considered to verify the system's performance under complex conditions.

Author Contributions: Conceptualization, W.C.; methodology, Z.L.; validation, H.S.; formal analysis, G.L.; investigation, B.Q. All authors have read and agreed to the published version of the manuscript.

Funding: This work is supported by the Jilin Province Science and Technology Development Project for the grant number 20220204138YY.

Institutional Review Board Statement: Not applicable.

Informed Consent Statement: Not applicable.

Data Availability Statement: The data presented in this study are available upon request from the corresponding author. The data are not publicly available due to privacy.

Acknowledgments: We thank all the authors for their support. The authors are also very grateful for the kind suggestions and valuable comments by the anonymous reviewers.

Conflicts of Interest: The authors declare no conflicts of interest.

References

1. Sutherland, W.; Emerson, J.; Dalton, G.; Atad-Ettedgui, E.; Beard, S.; Bennett, R.; Bezawada, N.; Born, A.; Caldwell, M.; Clark, P. The visible and infrared survey telescope for astronomy (VISTA): Design, technical overview, and performance. *Astron. Astrophys.* **2015**, *575*, A25. [CrossRef]
2. Jiang, L.J.; Ng, E.Y.K.; Yeo, A.C.B.; Wu, S.; Pan, F.; Yau, W.Y.; Chen, J.H.; Yang, Y. A perspective on medical infrared imaging. *J. Med. Eng. Technol.* **2005**, *29*, 257–267. [CrossRef]
3. Ring, E.; Ammer, K. Infrared thermal imaging in medicine. *Physiol. Meas.* **2012**, *33*, R33. [CrossRef]
4. Lahiri, B.B.; Bagavathiappan, S.; Jayakumar, T.; Philip, J. Medical applications of infrared thermography: A review. *Infrared Phys. Technol.* **2012**, *55*, 221–235. [CrossRef] [PubMed]
5. Cui, H.; Xu, Y.; Zeng, J.; Tang, Z. The methods in infrared thermal imaging diagnosis technology of power equipment. In Proceedings of the 2013 IEEE 4th International Conference on Electronics Information and Emergency Communication, Beijing, China, 15–17 November 2013; pp. 246–251.
6. Ren, C.C.; Li, P.J.; Chen, Z.X. Standard Target Simulation System for Infrared Thermal Imager. *Infrared Technol.* **2015**, *37*, 593–597.
7. Xia, T.Y.; Shuai, H.J.; Qiu, Y.F. Design of infrared target system for outfield. *J. Appl. Opt.* **2020**, *41*, 1067–1073.
8. Guo, Z.; Guan, W.; Wu, H. Multiscale Deblurred Feature Extraction Network for Automatic Four-Rod Target Detection in MRTD Measuring Process of Thermal Imagers. *Sensors* **2023**, *23*, 4542. [CrossRef] [PubMed]
9. Cao, M.; Cui, W.; Yao, Q. The Study on the MRTD Measurement System of Medical Infrared Thermal Imager Based on Sub-Pixel Edge Detection Algorithm. In Proceedings of the International Conference on Multimedia and Ubiquitous Engineering, Busan, Republic of Korea, 24–26 April 2016.
10. Singh, M.; Khare, S.; Kaushik, B.K. Objective evaluation method for advance thermal imagers based on minimum resolvable temperature difference. *J. Opt.* **2020**, *49*, 94–101. [CrossRef]
11. Gao, R.; Cai, Z. Object Detection in Thermal Infrared Image Based on Improved YOLOX. *IEEE Geosci. Remote Sens. Lett.* **2023**, *20*, 1–4. [CrossRef]
12. Meng, J.; Gao, H.; Ruan, M.; Guo, H.; Zhou, X.; Zhang, D. Design of vacuum annealing furnace temperature control system based on GA-Fuzzy-PID algorithm. *PLoS ONE* **2023**, *18*, e0293823. [CrossRef]
13. Chen, J.; Lu, Q.; Bai, J.; Xu, X.; Yao, Y.; Fang, W. A Temperature Control Method for Microaccelerometer Chips Based on Genetic Algorithm and Fuzzy PID Control. *Micromachines* **2021**, *12*, 1511. [CrossRef] [PubMed]
14. Tang, H.; Ma, R.; Chen, Y.; Huang, L.; Jiao, R. Temperature Regulation of Hot Vapor Preservation Treatment of Litchi Based on PSO-Fuzzy PID. *Appl. Sci.* **2023**, *13*, 6888. [CrossRef]
15. Ouyang, M.; Wang, Y.; Wu, F.; Lin, Y. Continuous Reactor Temperature Control with Optimized PID Parameters Based on Improved Sparrow Algorithm. *Processes* **2023**, *11*, 1302. [CrossRef]
16. Kasruddin Nasir, A.N.; Ahmad, M.A.; Tokhi, M.O. Hybrid spiral-bacterial foraging algorithm for a fuzzy control design of a flexible manipulator. *J. Low Freq. Noise Vib. Act. Control.* **2022**, *41*, 340–358. [CrossRef]

17. Jin, A.; Wu, H.; Zhu, H. Design of temperature control system for infant radiant warmer based on Kalman filter-fuzzy PID. *J. Phys. Conf. Ser.* **2020**, *1684*, 012140. [CrossRef]
18. Kumar, A.; Suhag, S. Whale Optimization Algorithm Optimized Fuzzy-PID Plus PID Hybrid Controller for Frequency Regulation in Hybrid Power System. *J. Inst. Eng. India Ser. B* **2022**, *103*, 633–648. [CrossRef]
19. Sun, Z.; Cao, Y.; Wen, Z.; Song, Y.; Sun, Z. A Grey Wolf Optimizer algorithm based fuzzy logic power system stabilizer for single machine infinite bus system. *Energy Rep.* **2023**, *9*, 847–853. [CrossRef]
20. Mishra, A.K.; Nanda, P.K.; Ray, P.K.; Das, S.R.; Patra, A.K. IFGO Optimized Self-adaptive Fuzzy-PID Controlled HSAPF for PQ Enhancement. *Int. J. Fuzzy Syst.* **2023**, *25*, 468–484. [CrossRef]
21. Zhang, H.; Zuo, X.; Sun, B.; Wei, B.; Fu, J.; Xiao, X. Fuzzy-PID-Based Atmosphere Packaging Gas Distribution System for Fresh Food. *Appl. Sci.* **2023**, *13*, 2674. [CrossRef]
22. Kherkhar, A.; Chiba, Y.; Tlemçani, A.; Mamur, H. Thermal investigation of a thermoelectric cooler based on Arduino and PID control approach. *Case Stud. Therm. Eng.* **2022**, *36*, 102249. [CrossRef]
23. Xie, Z.K.; Feng, K. Application of Improved Particle Swarm Fuzzy PID Algorithm in Temperature Control System. *Mech. Electr. Eng. Technol.* **2023**, *52*, 222–225.
24. Zhou, H.; Dong, L.; Zhan, M.K. Experimental and analysis on noise suppression and disturbance immunity of inverted pendulum stability based on genetic fuzzy PID algorithm. *J. Nav. Univ. Eng.* **2024**, 1–9.
25. Xue, J.; Shen, B. Dung beetle optimizer: A new meta-heuristic algorithm for global optimization. *J. Supercomput.* **2023**, *79*, 7305–7336. [CrossRef]
26. Pan, Z.Y.; Bo, F.L. DV-Hop localization algorithm optimized based on dung beetle optimizer. *J. Electron. Meas. Instrum.* **2023**, *37*, 33–41.
27. Alamgeer, M.; Alruwais, N.; Alshahrani, H.M.; Mohamed, A.; Assiri, M. Dung Beetle Optimization with Deep Feature Fusion Model for Lung Cancer Detection and Classification. *Cancers* **2023**, *15*, 3982. [CrossRef] [PubMed]
28. Jiao, Z.; Gao, S.; Liu, C.; Luo, J.; Wang, Z.; Lang, G.; Zhao, Z.; Wu, Z.; He, C. Digital Model of Plan View Pattern Control for Plate Mills Based on Machine Vision and the DBO-RBF Algorithm. *Metals* **2024**, *14*, 94. [CrossRef]
29. Guo, X.; Qin, X.; Zhang, Q.; Zhang, Y.; Wang, P.; Fan, Z. Speaker Recognition Based on Dung Beetle Optimized CNN. *Appl. Sci.* **2023**, *13*, 9787. [CrossRef]
30. Duan, J.; Gong, Y.; Luo, J.; Zhao, Z. Air-quality prediction based on the ARIMA-CNN-LSTM combination model optimized by dung beetle optimizer. *Sci. Rep.* **2023**, *13*, 12127. [CrossRef]
31. Zhu, F.; Li, G.; Tang, H. Dung beetle optimization algorithm based on quantum computing and multi-strategy fusion for solving engineering problems. *Expert Syst. Appl.* **2024**, *236*, 121219. [CrossRef]
32. Deng, Y.-Z.; Tang, S.-F.; Zeng, H.-Y.; Wu, Z.-Y.; Tung, D.-K. Experiments on Temperature Changes of Microbolometer under Blackbody Radiation and Predictions Using Thermal Modeling by COMSOL Multiphysics Simulator. *Sensors* **2018**, *18*, 2593. [CrossRef]
33. Tyler, R. Steiner, High temperature steady-state experiment for computational radiative heat transfer validation using COMSOL and ANSYS. *Results Eng.* **2022**, *13*, 100354.
34. Wu, A.G.; Wang, W.X.; Zhang, K.F.; Shen, S.N.; Duan, W.S.; Pan, R.; Luo, X. Multiphysics coupling analysis of heat pipe reactor based on Open MC and COMSOL Multiphysics. *Ann. Nucl. Energy* **2023**, *194*, 110115. [CrossRef]

Disclaimer/Publisher's Note: The statements, opinions and data contained in all publications are solely those of the individual author(s) and contributor(s) and not of MDPI and/or the editor(s). MDPI and/or the editor(s) disclaim responsibility for any injury to people or property resulting from any ideas, methods, instructions or products referred to in the content.